A 3D Imaging and Biological Marker Analysis of TMJ OA: A new Modeling Technique

David G. Walker

A thesis submitted to the faculty of the University of North Carolina at Chapel Hill in partial fulfillment of the requirements for the degree of Master of Science in the School of Dentistry (Orthodontics).

Chapel Hill
2013

Approved by:
Dr. Lucia Cevidanes

Dr. Tung Nguyen

Dr. Martin Styner

Abstract

DAVID G. WALKER: A 3D Imaging and Biological Marker Analysis of TMJ OA: A new Modeling Technique
(Under the direction of Dr. Lucia Cevidanes)

To investigate 3D morphology and biomarker profiles in a population of early onset TMJ Osteoarthritis (TMJ OA) subjects. Twelve subjects and controls underwent an exam and obtained a Cone beam CT (CBCT), as well as TMJ arthrocentesis and venipuncture. CBCT Datasets were used to construct 3D models of all condyles. Average OA and health models were created. 3D Shape Correspondence determined areas of statistically significant difference between models. Protein microarrays were used to analyze the synovial fluid (SF) and plasma samples. Shape Analysis MANCOVA was used to look for statistical correlations between biomarker levels and variations in surface morphology. The average OA model demonstrated a smaller size with areas of statistically significant difference. 32 biomarkers were measured in the plasma and/or SF samples. Shape Analysis MANCOVA successfully mapped variations in 10 SF and 20 plasma biomarkers to specific regions of anatomic variability in the OA group.

Table of Contents

List of Tables……iv

List of Figures……v

I. Introduction……1

II. A 3D Imaging Assessment of TMJ OA……3

2.1 Introduction……3

2.2 Methods……7

2.3 Results……11

2.4 Discussion……12

2.5 Conclusion……14

III. Local and Systemic Biomarkers in TMJ OA with an Integrated Biomolecular and 3D Model……21

3.1 Introduction……21

3.2 Methods……26

3.3 Results……31

3.4 Discussion……33

3.5 Conclusion……38

IV. References……48

List of Tables

A 3D Imaging Assessment of TMJ OA

Table 2.1: Subject and Control Demographics……15

Table 2.2: Oral and Maxillofacial Radiologists Findings for Subjects and Controls……16

Local and Systemic Biomarkers in TMJ OA with an Integrated Biomolecular and 3D Model

Table 3.1: Subject and Control Demographic……39

Table 3.2: The 50 Pre-selected Biomarkers of Interest……39

Table 3.3: 32 Biomarkers Detected in Either Plasma, Synovial Fluid or Both……40

Table 3.4: SF and Plasma Biomarkers associated with Morphologic variability and their General Functions……41

Table 3.5: Additional Plasma Biomarkers associated with Morphologic variability and their General Functions……42

List of Figures

A 3D Imaging Assessment of TMJ OA

Figure 2.1 Possible Continuum of Pathologic Change ……..17

Figure 2.2 Segmentation of the CBCT to Generate a 3D Model……..17

Figure 2.3: Establishing 25 Surface Points for Registering Condyle……..18

Figure 2.4: SPHARM mapping……..18

Figure 2.5: Comparison of OA Condyles and Average Control Model……..19

Figure 2.6: Comparison of the Mean Control and Mean OA Models……19

Figure 2.7: Anterior View of signed distance maps comparing individual OA and average control models……..20

Figure 2.8: Superior View of signed distance maps comparing individual OA and Average control models……20

Local and Systemic Biomarkers in TMJ OA and an Integrated Biomolecular and 3D Model

Figure 3.1: The Emerging Paradigm Shift in understanding, diagnosis, and treatment of OA……43

Figure 3.2: Comparison of the Average OA and Average Control Models……44

Figure 3.3: Results of Shape Analysis MANCOVA raw p-values for interactions between levels of SF Biomarkers and condylar morphology……44

Figure 3.4: Results of Shape Analysis MANCOVA raw p-values for interactions between levels of Plasma Biomarkers and condylar morphology (the same set of proteins demonstrated in Figure 3.3)……45

Figure 3.5: Results of Shape Analysis MANCOVA raw p-values for interactions between levels of the remaining Plasma Biomarkers and condylar morphology ……46

Figure 3.6: Shape Analysis MANCOVA p-values corrected with false discovery rate of 0.2 for interactions between levels of all Biomarkers and condylar morphology ……47

1. Introduction

Osteoarthritis is a common degenerative condition with an exploding prevalence estimated to double between 2000 and 2020.[1] The CDC estimates 13.9% of adults aged 25 and older and 33.6% of those over 65 are affected by OA.[7] In general, it is believed TMD symptoms, including limited range of motion, facial pain, and TMJ sounds, occur in 6 to 12 percent of the population, and based on the Research Diagnostic Criteria (RDC), 42.6% of patients with TMJ disorders present with evidence of TMJ OA.[8,9,10,11,12] Some have postulated that TMJ OA is the most common pathological condition of the TMJ.[13] Despite the prevalence of TMJ OA, the pathophysiological processes of this disease are still poorly understood.

The purpose of the first paper, *A 3D Imaging Assessment of TMJ OA*, was to qualitatively analyze condylar morphology in a group of clinically diagnosed TMJ OA subjects as compared to a group of non-OA controls. The specific aims were to: 1) generate 3D correspondent models of a group of subjects and controls; 2) generate an average model from the non-OA controls and an average model from the TMJ OA subjects; 3) utilize shape correspondence to detect areas of statistically significant differences between the two average models.

The purpose of the second paper, *Local and Systemic Biomarkers in TMJ OA with an Integrated Biomolecular and 3D Model,* was to evaluate the association between

morphologic characteristics and plasma and synovial fluid biomarkers in an early onset TMJ OA population, thereby initiating the process of developing a comprehensive OA model. Specifically, the aims of this study were: 1) determine local and systemic levels of pre-selected biomarkers in TMJ OA and control populations; 2) use Shape Analysis multivariate analysis of covariance (MANCOVA) to investigate potential correlations between variations in biomarker levels between the OA and control groups and variations in the morphology within the OA and control groups.

2. A 3D Imaging Assessment of TMJ OA

2.1 Introduction:

Osteoarthritis is a common degenerative condition with an exploding prevalence estimated to double between 2000 and 2020.[1] Because of the complex nature of this disease, therapeutic interventions have been limited primarily to analgesics and monitoring, with little existing evidence base for other treatment decisions.[1,2] Though commonly associated with knee, hip, and hand dysfunction, in the dental field, and in particular the Orofacial pain specialty, osteoarthritis of the temporomandibular joint (TMJ OA) has increased in focus as a form of temporomandibular joint disorder.

The term "temporomandibular disorder(s)" (TMD) refers to a myriad of specific conditions affecting the temporomandibular joint and associated structures, the muscles of mastication, or both. Though in clinical practice the generic term TMD is often used to describe all forms of disease/malfunction of the TMJ or associated structures, this is a drastic and dangerous oversimplification of an intricate group of conditions with inseparable organic and psychological components. The complexity in identifying, evaluating and treating the various forms of this complex group of disorders led to an effort to develop a diagnostic framework with a focus on providing a standardized assessment of the most common forms of TMD. The result of this project

was the establishment of the Research Diagnostic Criteria for Temporomandibular Disorders (RDC/TMD) which has been validated, modified, and critiqued in numerous studies and publications since first being published in 1992.[3, 4, 5, 6]

RDC/TMD is broadly divided into Axis I and Axis II diagnoses. Axis I is used to classify the physical pathological process or processes associated with a particular diagnosis, while Axis II classifies the psychological component of the disorder which is often paramount in diagnosis and treatment decisions. Axis I classifications include forms of muscle disorders, disc displacements, and degenerative joint diseases, the latter of which includes TMJ OA.

The CDC estimates 13.9% of adults aged 25 and older and 33.6% of those over 65 are affected by OA.[7] In general, it is believed TMD symptoms, including limited range of motion, facial pain, and TMJ sounds, occur in 6 to 12 percent of the population, and based on the Research Diagnostic Criteria (RDC), 42.6% of patients with TMJ disorders presented with evidence of TMJ OA.[8,9,10,11,12] Some have postulated that TMJ OA is the most common pathological condition of the TMJ.[13]

Like, many TMJ disorders, the symptomatic prevalence of OA differs greatly from the actual prevalence with only a fraction of patients complaining of pain or dysfunction.[14,15] While the absence of symptoms in the face of disease superficially seems benign or even beneficial for a patient, the reality is that such symptoms are useful in alerting a patient to seek medical attention, and without such an alarm, many patients fail to seek treatment until significant destruction has taken place.

Several classification schemes for describing OA degeneration have been described in the medical literature, however, it is unclear whether or not these systems are directly applicable to the TMJ, and given the uniqueness of the temporomandibular joint this should not be surprising.[6,16] Ahmed, et al have described a classification scheme for assessing the presence of OA changes in condyles and categorizing them as OA, indeterminate, or normal. In this system, a classification of indeterminate means there are some bony changes of the condyle consistent with OA, but not enough distinguishing features of the disease are present for a definitive diagnosis.[6]

Currently, diagnosis of TMJ OA focuses on the use of clinical exams and two-dimensional radiography; however, because of the great heterogeneity of TMJ OA and the diverse risk factors associated with the disease, identification is challenging.[1,5,8,17,18,19] Like in all cases, the use of conventional radiography in diagnosing TMJ OA is limited by the fact that it is a two-dimensional representation of a three-dimensional object and the superimposition of structures makes the diagnosis of early osteoarthritic defects impossible for all but the most skilled radiologist.

Cone-beam computed tomography (CBCT) is a rapidly advancing area of imaging with the capability to provide three dimensional images of hard and soft tissue structures, and has recently become the imaging modality of choice to study bony change in TMJ OA.[6,13,17,18,20-23]. As determined through the RDC/TMD validation project, revised clinical criteria alone without the use of imaging is inadequate for a valid diagnosis of OA. Furthermore, this project concluded that the prevalence of TMJ OA heretofore has been underestimated partially due to inadequate imaging techniques.[5,6]

TMJ OA is most commonly represented radiographically as flattening, erosions, scleroris, and osteophyte formation in the condylar head, as well as changes in the joint space and condylar fossa.[10,13,24] The increase in popularity of 3D imaging modalities, such as CBCT, in the dental field has greatly improved the ability of clinicians to visually assess many of these phenotypic characteristics of TMJ OA.[6,13,18,21]

Recently, the use of novel 3D imaging techniques using CBCT in conjunction with shape analysis using SPHARM-PDM has been validated for use in identifying and measuring simulated discrete, bony defects in condyles as well as in identifying various forms of osteoarthritic condylar changes such as flattening erosions and osteophyte formation and establishing a subjective possible continuum of pathologic change in TMJ OA (Figure 2.1).[17,20,22,23,25-27]

The focus of the present study was to objectively compare condylar morphology in a group of TMJ OA subjects to age and gender matched controls as determined by clinical diagnosis. Specifically, this study was implemented to do shape analysis of 3D surface models generated from CBCTs to investigate the specific phenotypic qualities of TMJ OA.

2.2 Methods:

Twelve subjects (average age 44.4 years) with a recent initial diagnosis of OA were recruited from the UNC Orofacial Pain and OMFS Clinics. Twelve controls (average age 41.3 years) were recruited through advertisement. All subjects were age and gender matched to a control (Table 2.1). Eleven females and one male were recruited for each group (91.7%% female), which is comparable to the 10:1 female to male ratio of TMD patients seen in the clinical setting, as reported in the literature.[8,9] All participants were between 21 and 66 years of age. Volunteers were excluded from the study based on the following criteria: refusal to consent to arthrocentesis or CBCT, history of malignancies, TMJ or jaw surgery, past trauma to the TMJ, intra-articular injection in the TMJ in the past 3 months, presence of a congenital craniofacial syndrome or anomaly, systemic condition involving the immune system, degenerative musculoskeletal or neuropathic sequelae, pregnancy, or a diagnosis of any form of arthritis of another joint in the body.

All participants underwent a comprehensive examination by an Orofacial pain specialist experienced in the use of the RDC/TMD protocol. Each exam included at least measurement of mandibular range of motion, palpation of the TMJ and muscles of mastication, evaluation of current pain status, and investigation of joint sounds. Based on the findings of this examination, and using the RDC/TMD guidelines, a subject was given a diagnosis of TMJ OA, a healthy TMJ, or inconclusive. An inconclusive diagnosis designated those individuals with pathology of the TMJ or associated structures that did

not appear to be osteoarthritic in origin. All subjects in this study were classified as having TMJ OA and all controls as having a healthy joint. Diagnosis of TMJ OA signs and symptoms would also include an opinion by the specialist as to whether the right or left TMJ was most affected. No radiographic images of any kind were used in making these determinations.

Following clinical examination, a Cone beam CT scan was obtained of all participants using a NewTom 3G imaging system. The NewTom 3G images patients in a supine position using a large field of view. The datasets obtained consist of approximately 300 axial cross-sectional slices with voxels reformatted to an isotropic 0.5x0.5x0.5mm.

All CBCTs were independently reviewed by two blinded, experienced oral and maxillofacial radiologists. Signs of flattening, localized sclerosis, generalized sclerosis, subchondral cysts, erosions, osteophytes, overall condylar resorption, and overall condylar proliferations were classified as absence, mild change, moderate change, or severe change. These results were used to apply the RDC guidelines for radiographic TMJ OA diagnosis, as described by Ahmad, et al., and a diagnosis was made for each subject.[6] These findings were not used to categorize participants as either OA or controls but were utilized at the completion of the study to help further elucidate the intricacies of the condylar morphology in these two groups.

CBCT datasets were de-identified and then converted from DICOM to ITK-compatible (Insight Segmentation and Registration Toolkit) format, specifically gipl format.[28] Using gipl files, 3D models were created through a process called

segmentation using the publicly available software ITK-Snap and utilizing methodologies adapted by Cevidanes, et al (Figure 2.2).[17,20,22,23,25-29] The process of segmentation has been described in detail elsewhere, and, in essence, consists of outlining the cortical boundaries of a desired region using manual and semi-automatic discrimination procedures to produce a 3D model that can be rotated 360 degrees in all directions.

After generating all 3D surface models, 24 for each group (48 total), left condyles were mirrored in the sagittal plane using image-converting software to form right condyles to facilitate comparisons. All condylar models were then cropped to a more defined region of interest consisting of only the condyle and a portion of the ramus. To approximate the condylar surfaces to one another in space, 25 surface points were selected on each condyle at corresponding (homologous) areas. The purpose of this registration was not to establish the final relationship of one model to the next, but to merely closely approximate the various anatomic regions of all condyles which have marked morphological variability. One observer identified 25 surface points on each condylar surface model: 4 points evenly spaced along the superior surface of the sigmoid notch, 4 on the medial and lateral portions of the ramus adjacent to the sigmoid notch, 3 along the posterior neck of the condyle, 3 on the medial and 3 on the lateral portion of the condylar neck, and on the medial, lateral, anterior, and posterior extremes of the condylar head (Figure 2.3).

After registration and normalization of the cropping areas across 3D models, binary segmentation volumes were created from the surface models. SPHARM-PDM

was then used to generate a mesh approximation from the segmentation volumes, whose points were mapped to a "spherical map". In that spherical map, parameterization of 4002 surface mesh points was optimized for each condylar model. The parameterization determines coordinate poles on each condylar model that allow the models to be related to one another in a consistent manner and identifies 4002 homologous or correspondent surface mesh points for statistical comparisons and detailed phenotypic characterization (Figure 2.4). Once the 4002 correspondent points were established for all individual condylar models, an average 3D condylar shape was generated for the TMJ OA group and control group. Comparisons were made between these two average models as well as between each individual OA model and the control average model. Statistical shape analysis was used to compare condylar morphologies, and differences between models were reported using vector distance maps and signed distance maps computed locally at each correspondent point (Figure 2.5).

2.3 Results:

Mean condylar models for both the TMJ OA and control groups produced a smoothly contoured surface. A comparison of means was performed for the two average models using multivariate analysis of covariance (MANCOVA).[30] The mean OA model was of smaller size in all dimensions and areas of statistically significant difference were localized to the anterior and superior portion of the lateral pole, as well as the anterior, superior, and medial portions of the medial pole (Figures 2.6).

Commonly, the individual OA models demonstrated areas of bony excess and deficiency in comparison to the average control model, and great variability between the individual models was evident (Figure 2.7, 2.8).

In the examination of the Cone beam CT datasets by the OMF Radiologists, only one condyle was classified as healthy, 8.3% of the study population. Radiographically, 35.4% of condyles were classified as indeterminate, and 56.3% as having signs of OA. These radiographic results are in comparison to the clinical diagnosis, which by design consisted of 50% OA and 50% normal. Flattening was the most prevalent finding, evident in 85.4% of the study population. In the OA group, 70.8% of condyles were given a radiographic diagnosis of OA while 25% were indeterminate based on the RDC criteria. For the control group, 41.7% of condyles were classified as having OA, 4.58% as indeterminate and 12.5% as normal (Table 2.2).

Discussion:

This investigation provided detailed information on the radiographic findings of an early onset TMJ OA and a clinically healthy control population. Characteristic areas of bony excess and deficiency were identified in the OA population, and localized for each specific case. Wide variation existed in both the OA and control groups in both overall condylar size and shape. Vector and signed distance maps proved successful in allowing easy visualization of the individual variation in both groups.

Average OA and control models were successfully generated. The average OA model was found to have a smaller overall morphology with areas of statistically significant difference localized to various regions of the medial and lateral poles.

Perhaps one of the most surprising findings in this study was the high incidence of OA signs and even radiographic diagnosis of OA in both the OA group and the control group. Individuals included in the control group reported no signs or symptoms of TMJ dysfunction and were given a clinical diagnosis of a healthy joint. The discrepancy in the clinical and radiographic findings underscores the need for a combined clinical and radiographic assessment in evaluating the TMJ for diseases such as osteoarthritis as well as the often surreptitious nature of early OA.

The increased popularity of CBCT in the dental setting has met with some criticism of late. Some argue the data acquired using a large field of view is more than what is needed for most dental procedures and therefore the routine use of such imaging is in violation of the ALARA (as low as reasonably achievable) principle espoused by OMF radiologists. However, one can hardly argue with the increased

diagnostic capabilities provided the clinician in certain cases. In the development of a phenotypic library and comprehensive phenotypic description of TMJ OA, CBCT will likely prove indispensable as the ability to view condylar morphology in 3D is becoming critical for the accurate assessment of these joints.

Previous studies which utilized 2D radiography were forced to rely on subjective grading scales which were often modified from those present in the medical literature and varied from study to study. The use of 3D models and shape analysis allows one to make localized quantitative measurements of the bony changes which have taken place while minimizing subjective factors and eliminating the problem of superimposition which is inescapable when using 2D methods. By using 3D surface models, this study has undoubtedly provided a more accurate description of TMJ OA morphology than previously described.

Ultimately, this study has served to expound on the present knowledge regarding the morphologic variability in TMJ OA and to further elucidate some of the intricacies associated with osteoarthritic destruction in the temporomandibular joint. This new evidence will aid the development of more precise classifications of this condition and help pave the way for future studies investigating genetic and biochemical aspects of this disease in a more targeted manner than previously possible.

2.5 Conclusions:

In summary, the following conclusions can be drawn from this investigation:

1. There was great variability in individual condylar morphology seen in both the OA and control groups.
2. There was a trend for OA condyles to demonstrate bony excess on the anterior surface and bony deficiency on the superior surface of the condylar head, with respect to the average control model.
3. The mean OA model had a smaller overall morphology with areas of statistically significant difference localized to the regions of the lateral and medial poles.
4. Despite a thorough clinical exam to divide participants into OA and control groups, radiographic signs of OA were still detected in both groups.

Table 2.1: Subject and Control Demographics

	Subjects		Controls		
M/F	ID	Age (years)	Age (years)	ID	Age Difference (years)
F	O1	51	44	C1	7
F	O6	66	65	C2	1
F	O3	61	49	C3	12
F	O4	29	29	C7	0
F	O9	62	57	C6	5
F	O15	51	39	C4	12
M	O8	36	36	C8	0
F	O12	46	44	C9	2
F	O10	38	39	C10	1
F	O11	26	29	C11	3
F	O13	21	22	C13	3
F	O14	46	43	C14	3
Average		44.4	41.3		4.1

Table 2.2: OMFR Findings for Subjects and Controls

Condyle	Subject	Radiographic Impression		Control
Left	O1	OA	OA	C1
Right		OA	OA	
Left	O6	OA	Indeterminate	C2
Right		OA	Indeterminate	
Left	O3	OA	Indeterminate	C3
Right		OA	Indeterminate	
Left	O4	OA	Indeterminate	C7
Right		OA	Indeterminate	
Left	O9	OA	OA	C6
Right		OA	OA	
Right	O15	OA	OA	C4
Left		Healthy	OA	
Left	O8	Indeterminate	Indeterminate	C8
Right		Indeterminate	Indeterminate	
Left	O12	OA	OA	C9
Right		OA	OA	
Left	O10	OA	Indeterminate	C10
Right		Indeterminate	Indeterminate	
Left	O11	Indeterminate	Healthy	C11
Right		Indeterminate	Healthy	
Left	O13	Indeterminate	Indeterminate	C13
Right		OA	Healthy	
Left	O14	OA	OA	C14
Right		OA	OA	
Percent		OA: 70.8% Indeterminate: 25% Healthy: 4.2%	OA: 41.7% Indeterminate: 45.8 Healthy: 12.5%	

Figure 2.1: Possible continuum of pathologic change generated using 3D surface models from CBCT images.[23]

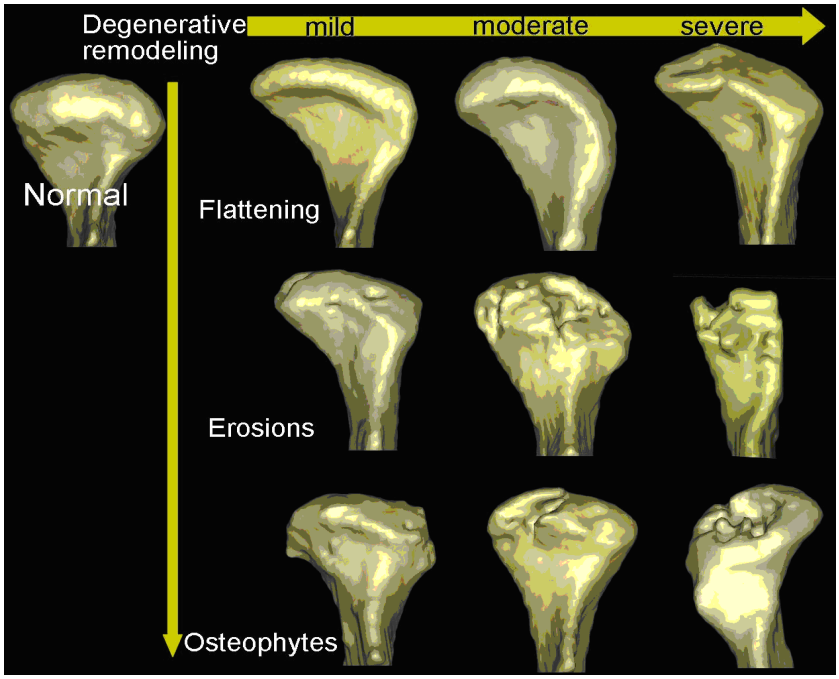

Figure 2.2: Segmentation of the CBCT to generate a 3-D model.

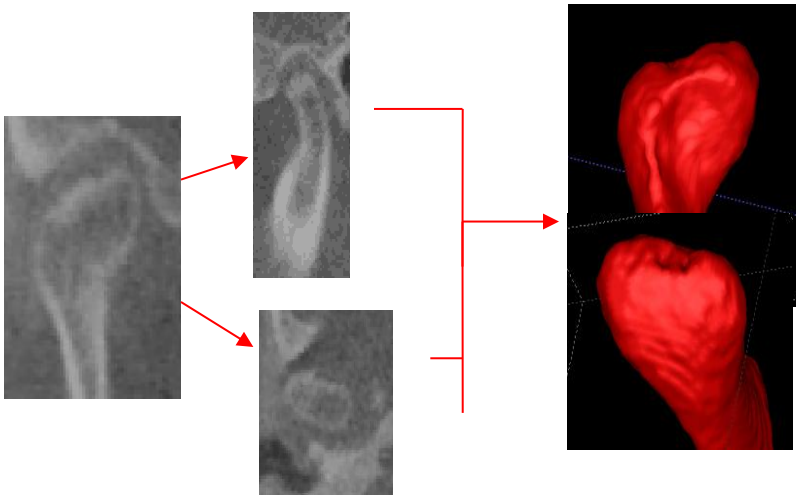

Figure 2.3: Establishing 25 surface points for registering condyles

Figure 2.4: SPHARM-PDM mapping coordinates the 4002 surface points in the mesh models to individual points on a spherical map for each 3D segmentation model.

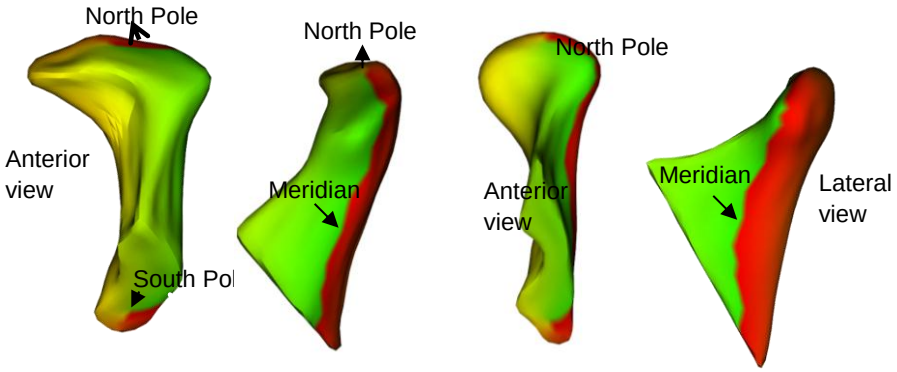

Figure 2.5: (left) Alignment of an OA condyle (grey) and the average control model (red) using the SPHARM-PDM correspondent points. (right) Signed difference maps depicting areas of morphologic difference between the average control model and an individual OA model (red represents bony excess and blue represents bony deficiency of the OA model with respect to the control average

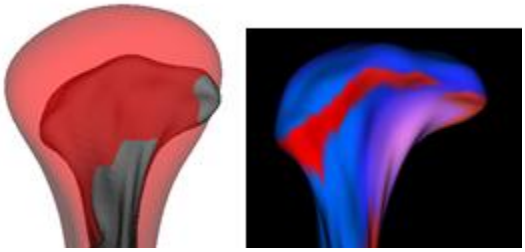

Figure 2.6: Comparison of the mean control and mean OA models. Color maps depict areas of statistically significant difference ($p<0.05$).

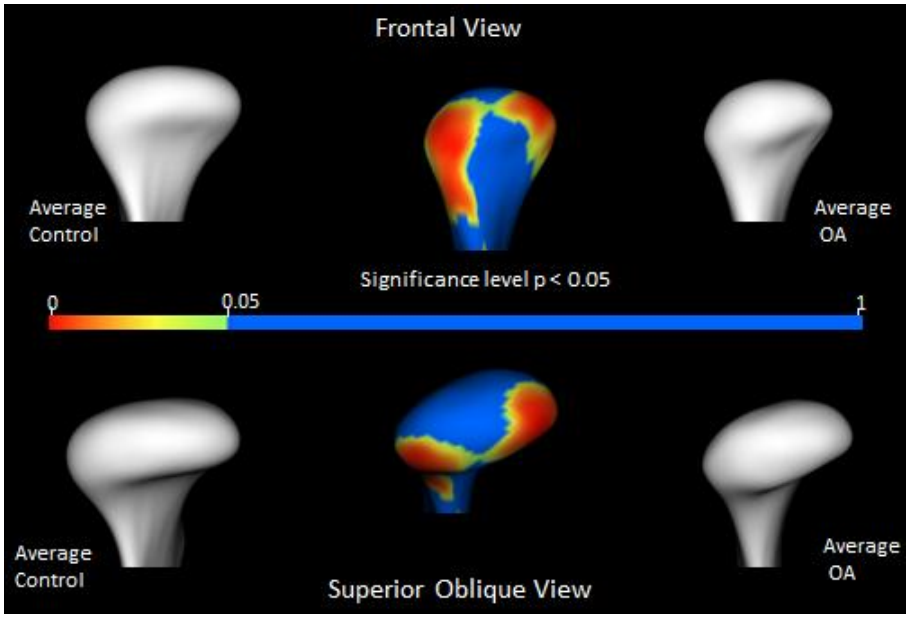

Figure 2.7: Anterior view of signed distance maps comparing individual OA and average control models.

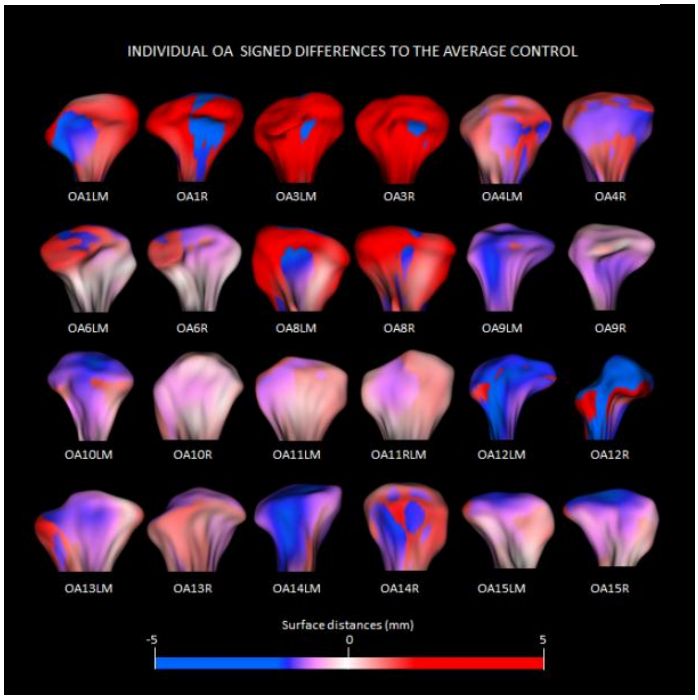

Figure 2.8: Superior view of signed distance maps comparing individual OA and average control models.

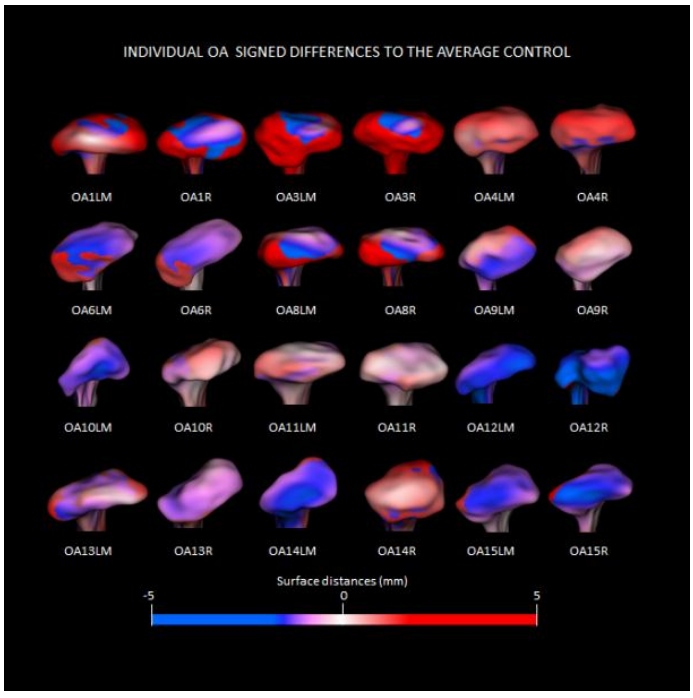

3. Local and Systemic Biomarkers in TMJ OA and an Integrated Biomolecular and 3D Model

3.1 Introduction

Osteoarthritis is one of the leading causes of disability with symptomatic knee OA being present in 13% of persons over 60 year of age.[31] According to the Research Diagnostic Criteria (RDC), 42.6% of patients with TMJ disorders present with evidence of TMJ OA.[6,4,5,19]

Subchondral bone remodeling plays an important role in the pathogenesis of OA.[32] While OA has been primarily known as a cartilage disorder, this disease also involves early increases in the subchondral bone remodeling and subsequent osteophyte formation.[33, 34] An important emerging theme in osteoarthritis is a broadening of focus from a disease of cartilage to one of the 'whole joint'. Its etiology is largely unknown, but is most likely multi-factorial. A variety of etiologic risk factors and pathophysiologic processes contribute to the progressive nature of the disease and serve as targets of behavioral and pharmacologic interventions. Risk factors such as age, sex, trauma, overuse, genetics, and obesity can each make contributions to the process of degeneration in different compartments of the joint. Such risk factors can serve as initiators that promote abnormal biochemical processes involving the cartilage, bone, and synovium, with cross-talk among molecular mediators in these

components of the joint, which over a period of years result in the characteristic features of OA: degradation of articular cartilage, osteophyte formation, subchondral sclerosis, disc degeneration, bone lesions, and synovial proliferation.[33]

Because adult cartilage is both avascular and aneural, it is possible for extensive damage to take place in a joint space like the TMJ before a patient complains of symptoms of the disorder. The great challenge in understanding and treating osteoarthritis is that it often begins attacking different joint tissues long before middle age, but cannot be diagnosed until it becomes symptomatic decades later, at which point structural alterations are already quite advanced. No proven disease-modifying therapy exists for osteoarthritis and current treatment options for chronic osteoarthritic pain are insufficient.[35]

Currently, diagnosis of TMJ OA focuses on the use of clinical exams and two-dimensional radiography; however, because of the great heterogeneity of TMJ OA and the diverse risk factors associated with the disease, identification and treatment is challenging.[1, 2, 14, 36-41] Like in all cases, the use of conventional radiography in diagnosing TMJ OA is limited by the fact that it is a two-dimensional representation of a three-dimensional object and the superimposition of structures makes the diagnosis of early osteoarthritic defects such as erosions or osteophyte formation impossible for all but the most skilled radiologist.

Cone beam computed tomography (CBCT) is a rapidly advancing area of imaging with the capability to provide three dimensional images of hard and soft tissue structures, and CBCT has recently become the imaging modality of choice to study bony

change in TMJ OA.[13, 18, 21, 22, 42-44] As determined through the RDC/TMD validation project, revised clinical criteria alone without the use of imaging is inadequate for a valid diagnosis of OA. Furthermore, this project concluded that the prevalence of TMJ OA heretofore has been underestimated partially due to inadequate imaging modalities.[45-47]

Recently, the use of novel 3D imaging techniques using CBCT in conjunction with SPHARM-PDM shape analysis has been validated for use in identifying and measuring simulated discrete, bony defects in condyles as well as being used to identify various forms of osteoarthritic condylar changes such as flattening erosions and osteophyte formation and establishing a possible continuum of pathologic change in TMJ OA.[17, 23, 25, 26, 48]

Biomarkers have been defined as "objective indicators of normal biologic processes, pathogenic processes, or pharmacologic responses to therapeutic interventions."[31] The shift towards focusing on biomarker levels as indicators of physiologic or pathophysiologic processes represents a true paradigm shift in the study of TMJ OA. The NIH-funded OA Biomarkers Network established a system for categorizing OA biomarkers known as the BIPED system, where BIPED stands for burden of disease, investigative, prognostic, efficacy of intervention, and diagnostic.[31] Over 100 cytokine mediators of various aspects of OA, such as nociception and bone resorption, have been identified.[8, 15, 40, 41, 49-59] The recent work of Slade et al suggests that not only local synovial fluid may play a role in the cross-talk among the different joint tissues, but also circulating levels of pro-inflammatory cytokines and more

generalized systemic processes may contribute to the pathophysiology of disorders of the temporomandibular joint.[60] Cytokines are proteins synthesized by nearly all nucleated cells that are in turn capable of responding to them.[61] Their synthesis is initiated by gene transcription and their mRNAs are short lived. They are produced as needed in immune responses. Individual cytokines are produced by and act on many cell types (i.e., they are pleiotropic) and in many cases cytokines have similar actions (i.e., they are redundant).

With three affected tissues in TMJ OA, cartilage, bone and synovium, it is unlikely one biomarker will provide a comprehensive description of this intricate disease.[31, 40, 59, 62] It will be the goal of this study to work towards a paradigm shift from looking for one specific biomarker to identify a disease process to the concept of looking for sets of biomarkers to categorize a complex disease.[63] The ability to identify biomarkers associated with early-onset OA may lead to the ability to identify patients at risk for developing more severe stages of the disease and highlight targets for future mechanism-based therapies.

The implications for providing a comprehensive model of a complex disease process such as TMJ OA that integrates clinical, morphological and biomolecular assessments are far reaching. Establishing connections between specific biomarker data and 3D imaging will possibly result in treatment modalities more specifically targeted towards the prevention or even reversal of joint destruction.

The aim of the second portion of this two part pilot study was to elucidate contributions of various biomarkers to characteristic phenotypes of an early onset

temporomandibular joint osteoarthritis population, while advancing towards developing a comprehensive OA model. We hypothesized that variations in cytokine protein levels would correspond with the pattern of resorption of the supero-lateral surface of the condyles and the bone apposition in the mid-anterior surface of the condyles that are characteristic of condylar morphology in TMJ OA. To test these hypotheses, we determined associations of (1) circulating cytokines with condylar morphology and case status of OA and healthy controls; and (2) synovial fluid cytokines with condylar morphology and case status of OA and healthy controls. Specifically, we aimed to evaluate the association between morphologic characteristics and plasma and synovial fluid biomarkers in an early onset TMJ OA population, thereby initiating the process of developing a comprehensive OA model (Figure 3.1).

3.2 Methods:

Twelve subjects (average age 44.4 years) with a recent initial diagnosis of OA were recruited from the UNC Orofacial Pain and OMFS Clinics. Twelve controls (average age 41.3 years) were recruited through advertisement. All subjects were age and gender matched to a control (Table 3.1). Eleven females and one male were recruited for each group (91.7%% female), which is comparable to the 10:1 female to male ratio of TMD patients seen in the clinical setting, as reported in the literature.[8, 9] All participants were between 21 and 66 years of age. Volunteers were excluded from the study based on the following criteria: refusal to consent to arthrocentesis or CBCT, history of malignancies, TMJ or jaw surgery, past trauma to the TMJ, intra-articular injection in the TMJ in the past 3 months, presence of a congenital craniofacial syndrome or anomaly, systemic condition involving the immune system, degenerative musculoskeletal or neuropathic sequelae, pregnancy, or a diagnosis of any form of arthritis of another joint in the body.

All participants underwent a comprehensive examination by an Orofacial pain specialist experienced in the use of the RDC/TMD protocol. Each exam included at least measurement of mandibular range of motion, palpation of the TMJ and muscles of mastication, evaluation of current pain status, and investigation of joint sounds. Based on the findings of this examination, and using the RDC/TMD guidelines, a subject was given a diagnosis of TMJ OA, a healthy TMJ, or inconclusive. An inconclusive diagnosis designated those individuals with pathology of the TMJ or associated structures that did not appear to be osteoarthritic in origin. All subjects in this study were classified as

having TMJ OA and all controls as having a healthy joint. Diagnosis of TMJ OA signs and symptoms would also include an opinion by the specialist as to whether the right or left TMJ was most affected. No radiographic images of any kind were used in making these determinations.

Following clinical examination, a Cone beam CT scan was obtained of all participants using a NewTom 3G imaging system. The NewTom 3G images patients in a supine position and using a large field of view. The datasets obtained consist of approximately 300 axial cross-sectional slices with voxels reformatted to an isotropic 0.5x0.5x0.5mm.

CBCT datasets were de-identified and then converted from DICOM to ITK-compatible (Insight Segmentation and Registration Toolkit) format , specifically gipl format.[28] Using gipl files, 3D models were created through a process called segmentation using the publicly available software ITK-Snap and utilizing methodologies adapted by Cevidanes, et al.[17,20,22,23,25-29] The process of segmentation has been described in detail elsewhere, and, in essence, consists of outlining the cortical boundaries of a desired region using manual and semi-automatic discrimination procedures to produce a 3D model that can be rotated 360 degrees in all directions.

Models were generated of the condyle sampled using arthrocentesis (the more affected condyle of each OA subject), for a total of 24 condyles. After generating all 3D surface models, left condyles were mirrored in the sagittal plane using image-converting software to form right condyles to facilitate comparisons. All condylar models were then cropped to a more defined region of interest consisting of only the

condyle and a portion of the ramus. To approximate the condylar surfaces to one another in space, 25 surface points were selected on each condyle at corresponding (homologous) areas. The purpose of this registration is not to establish the final relationship of one model to the next, but merely closely approximate the various anatomic regions of all condyles which present marked morphological variability. One observer identified 25 surface points on each condylar surface model: 4 points evenly spaced along the superior surface of the sigmoid notch, 4 on the medial and lateral portions of the ramus adjacent to the sigmoid notch, 3 along the posterior neck of the condyle, 3 on the medial and 3 on the lateral portion of the condylar neck, and on the medial, lateral, anterior, and posterior extremes of the condylar head .

After registration and normalization of the cropping areas across 3D models, binary segmentation volumes were created from the surface models. SPHARM-PDM was then used to generate a mesh approximation from the segmentation volumes, whose points were mapped to a "spherical map". In that spherical map, parameterization of 4002 surface mesh points was optimized for each condylar model. The parameterization determines coordinate poles on each condylar model that allow the models to be related to one another in a consistent manner and identifies 4002 homologous or correspondent surface mesh points for statistical comparisons and detailed phenotypic characterization. Once all individual condylar models had 4002 correspondent points, an average 3D condylar shape was generated for the TMJ OA group and control group.

TMJ arthrocentesis was performed by an experienced OMF surgeon using a validated protocol.[65-73] The joint chosen for arthrocentesis was selected based on the opinion of the pain specialist as to which joint was most affected. If both joints are equally affected, or if neither joint appeared to be affected (as with the control patients), the right joint was chosen. Arthrocentesis was performed using a push/pull technique in which 4ml of a saline solution was injected into the joint and then 4ml of solution withdrawn under local anesthesia. The saline solution consisted of 78% saline and 22% hydroxocobalamin, which is included in order to determine the volume of synovial fluid recovered in the aspirate by comparing the spectrophotometric absorbance of the aspirate with that of the washing solution. Venipuncture was performed on the median cubital vein of each patient's left arm and 5ml of blood was obtained. Intravenous sedation for the aforementioned procedures was offered to each participant.

Custom quantibody protein microarrays (RayBiotech) were used to evaluate the synovial fluid and plasma samples for 50 biomarkers. The biomarkers chosen were known to be associated with bone repair and degradation, inflammation or nociception, common processes seen in OA. Quantibody arrays use pairs of antibodies to capture the protein of interest, similar to an ELISA assay. The use of biotinylated antibodies and a streptavidin-conjugated fluor allow detection levels for the specific proteins to be visualized using a fluorescence laser scanner.[74] Preprocessing steps for these samples were completed at the University Of Michigan School Of Dentistry and then shipped to RayBiotech (Norcross, GA) for analysis. All samples were measured in duplicate using 2 separate slides with 19 and 31 proteins respectively, to control for proteins with

cross-reactivity (Table 3.2). Shape analysis MANCOVA (Multivariate Analysis of Covariance) was used to test interactions between protein levels and individual condylar morphology in the OA subjects' plasma and synovial fluid samples.[30] Shape analysis MANCOVA operates by testing the Pearson Correlations between alterations in each of the various biological marker levels and differences in each one of the correspondent 4002 surface points obtained with SPHARM-PDM in the morphology of each of the control and OA condyles with p-values significance set at 0.05. Because the condylar surface mesh data is recorded in three dimensions (x, y, and z) at 4002 locations, and the sample size is only 12 condyles in each group, which represents high dimensional low sample size data, these findings are corrected for multiple comparisons using a false discovery rate of 0.2.

3.3 Results:

Of the 50 biomarkers, the levels of 32 were consistently measured within the standard curve of detection in either blood and/or synovial fluid as presented in Table 3.3. Proteins levels below the limit of detection in either blood and/or synovial fluid are shown with red borders. Ten synovial fluid biomarkers and one serum biomarker highlighted in Table 3.3 demonstrated close to two-fold or greater variation between the OA and control groups. Because of the high variability in detection levels and small sample size of 12 matched pairs, median values rather than mean values for the biomarker detection levels are presented.

Of the 32 proteins detected above threshold, associations with the variability in condylar morphology at specific anatomic regions ($p < 0.05$) shown by Pearson Correlation color maps using the MANCOVA analysis were observed for 22 proteins: 10 in the synovial fluid, 8 of these same proteins in plasma, and another 12 proteins in plasma samples (Figures 3.3- 3.5). The general functions of these proteins are presented in Table 3.4 and Table 3.5.

In the synovial fluid of patients with a clinical diagnosis of OA, 6ckine and ENA-78 levels showed small areas of correlations with morphological differences in the lateral pole morphology. ANG, GDF15, TIMP-1, CXCL16, MMP-7 and MMP-3 showed small areas of correlations with morphological differences in the anterior surface of the condyle. MMP-3 levels were more than 2 fold lower in OA compared to controls in synovial fluid and presented significant correlations with condylar surfaces that present bone proliferation. ENA-78, CXCL14 and MMP-9 levels were correlated to morphological differences in the posterior surface of the condyle. Statistically

significant correlations in the control group were observed in much smaller and different anatomic areas than in the OA group. Only ENA-78 still presented significant correlations when the findings were corrected for false discovery rate of 0.2 (Figure 3.6).

In the plasma of patients with clinical diagnosis of OA, ANG and GDF15 levels were significantly correlated with morphological differences in the anterior surface of the condyle. CXCL14 levels were correlated to morphological differences in the posterior surface of the condyle. 6ckine, ENA-78, TIMP-1, CXCL16, MMP-3, PAI-1, VE-Cadherin, VEGF, MIP-1b, EGF, GM-CSF, TGFb1, TNFa, IFNg, IL-1a, IL-6 and BDNF levels were significantly correlated to morphological variability in the latero-superior surface of the condyle. ENA-78, MMP-3, PAI-1, VE-Cadherin, VEGF, GM-CSF, TGFb1, IFNg, IL-1a and IL-6 levels still presented significant correlations when the findings were corrected for false discovery rate of 0.2 (Figure 3.6).

In the control subjects for both synovial fluid and plasma samples, the protein levels presented small interactions with condylar morphology that were not present with false discovery rate correction except for ANG in plasma. ANG plasma levels were significantly correlated with the superior surface of the condyle (p-value < 0.05) and even when corrected for a false discovery rate of 0.2 (Figures 3.4 and 3.6).

3.4 Discussion:

This study is the first to report a statistically significant association between specific OA biomarkers and TMJ condylar surface morphological variability at specific anatomic regions in 3D. Advances in proteomics and 3D shape analysis have brought expectations for application of increased knowledge about mechanisms of osteoarthritis toward more effective and enduring therapies. This study highlights metrics and methods that may prove instrumental in charting the landscape of evaluating individual molecular and imaging markers so as to improve diagnosis, prognosis, and mechanism-based therapy.

In the first part of this two-part investigation we aimed to improve the understanding of the morphology of TMJ OA through the use of 3D models and shape correspondence. The results of that study included the description of distinct regions of statistically significantly different morphology between a mean OA and mean control model developed from clinically diagnosed OA and healthy groups. This study also demonstrated an overall smaller condylar average for the OA group as compared to the control average and great variability in individual condylar form.

The second part of this investigation aimed to use systemic (plasma) and local (synovial fluid) fluid samples to detect levels of known inflammatory biomarkers and then correlate those biomarkers which were altered in the disease state to 3D models of OA derived in part one. The semi-transparent overlays and signed distances between average OA and control condylar models, in Figure 3.2, revealed that bone apposition/reparative proliferation, shown as the white areas in the antero-superior surface of the OA condyle, were characteristic of OA morphology , leading to variability

in condylar torque in OA patients. Bone resorption was more marked in the latero-superior surfaces of the condyles.

In the synovial fluid samples, two of the most striking results of the MANCOVA analysis show that the levels of MMP-3 in synovial fluid, that were ~2 fold lower in the OA group compared to the controls, were correlated to areas of bone apposition/reparative proliferation that occurs in the anterior surface of the condyles, and ENA-78 was strongly correlated ($p<0.01$) to changes in the lateral pole and the posterior surface of the medial pole in the TMJ OA group (Figure 3.3).

As a member of the chemokine family, CXCL14/BRAK induces chemotaxis of monocytes, however it has been suggested that it is involved more in the homeostasis of monocyte-derived macrophages, which are associated with pathologic changes in OA.[75] It is interesting to note that in this study local and systemic levels of CXCL14/BRAK show the same pattern of morphologic correlations (Figures 3.3. and 3.4).

The biomarkers for which no association with morphology was established serve various physiologic and pathophysiologic processes and have been implicated in other studies as playing a role in arthritis.[59, 81] For example, MMP-2, which demonstrated differences in detection level between the OA and control groups in the synovial fluid, is involved in the degradation of type IV collagen, the major structural component of basement membranes and plays a role in the inflammatory response.[75] Neither of these processes necessarily correlate to bony changes in OA, but might be more involved in the pathology of associated tissues (ie. the lining of the synovial membrane).

Also, TIMP-2, which again was elevated in the synovial fluid samples for the OA

group, is an inhibitor of MMPs, and is thought to be critical in maintaining tissue homeostasis through interactions with angiogenic factors and by inhibiting protein breakdown processes, an activity associated with tissues undergoing remodeling of the ECM.

Interestingly, protein level measurements were much higher in plasma than in synovial fluid. It could be questioned that arthritis localized in small joints such as the TMJs may not lead to changes in systemic levels of proteins and that possibly undiagnosed arthritis of other joints in the body may be confounders in plasma protein expression. However, systemic levels in plasma of proteins in OA patients were significantly correlated with condylar morphologic variability, as shown in figures 3.4 to 3.6. The most striking patterns of interactions was between levels of 17 proteins in plasma with the resorption in the antero-superior surfaces of condylar lateral pole as shown in Figures 3.4 and 3.5.: 6ckine, ENA-78, TIMP-1, CXCL16, MMP-3, PAI-1, VE-Cadherin, VEGF, MIP-1, EGF, GM-CSF, TGFb1, IFNg, TNFa, IL-1a, IL-6 and BDNF. Because these pilot study findings represent high dimensional low sample size data, after correction of findings using a false discovery rate of 0.2, ENA78, MMP3, PAI1, VE-Cadherin, VEGF, GM-CSF, TGFb1, IFNg, IL-1a and IL-6 levels still presented significant correlations which indicates that 20% of the significant locations of interactions are expected to be falsely significant, but the overall pattern represents the interaction protein levels and morphology (Figure 3.6).

In the control subjects both in synovial fluid and plasma, protein levels presented small interactions with condylar morphology in condylar surface regions that differ from the OA group. However, those small interactions cannot be verified when

use false discovery rate correction. ANG levels were significantly correlated with the superior surface of the condyle (p-value < 0.05) even when corrected for false discovery of 0.2 (Figures 3.4 and 3.6).

This investigation limited inclusion in the OA group to those individuals with a recent diagnosis and onset. Several of the biomarkers investigated did not demonstrate significantly variable expression between the two groups, and those for which no morphological association could be established, have been previously investigated by other groups and found to be associated with clinical diagnosis of OA, either in the TMJ or another joint. It is possible that by limiting this investigation to recent onset OA, the disease had not progressed to a stage where these biomarkers play as paramount of a role.

A limitation of this pilot study was the inability to test biomarkers in pairs or groups to evaluate whether or not there is cross-reactivity between them that is associated with condylar morphology. This should be an aim of future investigations in this area, as testing biomarkers in groups or pairs will likely be a more accurate representation of the in vivo state.[38] However, the study of 50 proteins, expressed in previous studies of the complex clinical conditions of inflammation, angiogenesis and neuroception that may lead to bone resorption and/or reparative proliferation in osteoarthritis, revealed that 22 cytokines presented interactions with morphological variability.

In summary, 22 cytokines presented interactions with early signs of bone remodeling in the articular surfaces of the condyles that are already observed at the first clinical diagnosis. The levels of MMP-3 in synovial fluid, that were ~2 fold lower in

the OA group compared to the controls, were correlated to the bone apposition that occurs in the anterior surface of the condyles and leads to characteristic changes in condylar torque and morphology. Other proteins in plasma and synovial fluid that may play a role in the bone apposition of the anterior surface of the condyles include ANG, GDF15, TIMP-1, CXCL16 and MMP-7. Bone resorption with flattening and reshaping of the lateral pole of the condyle involves molecular pathways with interaction of 17 proteins measured in this study: 6ckine, ENA-78, TIMP-1, CXCL16, MMP-3, PAI-1, VE-Cadherin, VEGF, MIP-1, EGF, GM-CSF, TGFb1, IFNg, TNFa, IL-1a, IL-6 and BDNF.

3.5 Conclusions:

1. This study developed a protocol for mapping statistically significant interactions between alterations in biomarker levels and alterations in condylar morphology in a clinically diagnosed TMJ OA population.
2. A total of 22 biomarkers demonstrated a statistically significant association with morphologic variability as determined using the MANCOVA analysis (10 biomarkers from the synovial fluid sample, and 10 of the same proteins plus an additional 12 from the plasma sample).
3. Levels of ANG, GDF15, TIMP-1, CXCL16, MMP-3 and MMP-7 presented interactions with the bone apposition of the anterior surface of the condyles.
4. Levels of 6ckine, ENA-78, TIMP-1, CXCL16, MMP-3, PAI-1, VE-Cadherin, VEGF, MIP-1, EGF, GM-CSF, TGFb1, IFNg, TNFa, IL-1a, IL-6 and BDNF presented interactions with bone resorption and flattening reshaping of the lateral pole of the condyle.

Table 3.1: Subject and Control Demographics

	Subjects		Controls		
M/F	ID	Age (years)	Age (years)	ID	Age Difference (years)
F	O1	51	44	C1	7
F	O6	66	65	C2	1
F	O3	61	49	C3	12
F	O4	29	29	C7	0
F	O9	62	57	C6	5
F	O15	51	39	C4	12
M	O8	36	36	C8	0
F	O12	46	44	C9	2
F	O10	38	39	C10	1
F	O11	26	29	C11	3
F	O13	21	22	C13	3
F	O14	46	43	C14	3
Average		44.4	41.3		4.1

Table 3.2: Separate slides of microarrays to measure 50 proteins while controlling for cross-reactivity

19 protein slide		31 protein slide		
aFGF	MMP-3	6ckine	IFNg	NT-4
ANG	MMP-7	bFGF	IGF-I	OPG
BDNF	MMP-9	BLC	IL-1a	TGF-b1
BMP-2	NT-3	CXCL16	IL-1b	TGF-b2
CXCL14/BRAK	PAI-I	EGF	IL-6	TGF-b3
GDNF	RANK	ENA-78	LIF	TIMP-2
ICAM-1	TIMP-1	FGF-7	MCP-1	TNFa
ICAM-3	VE-Cadherin	G-CSF	MIP-1a	TNFb
MIP-1b		GDF-15	MMP-1	VEGF
MMP-10		GM-CSF	MMP-13	
MMP-2		HB-EGF	NGF R	

Table 3.3: Median levels for Serum and SF. Levels below the limit of detection are shown with red borders and variations of approximately 2x or greater between groups are highlighted

Biomarker	Serum Data		Synovial Fluid Data		*Limit of Detection*	*Highest Standards*
	Control Median	OA Median	Control Median	OA Median		
ANG	2,070.90	1,952.20	350.5	884.5	1.22	3,000.00
BDNF	6,616.40	4,761.50	0.9	4.5	11.03	15,000.00
BMP-2	5,331.30	5,304.20	2,085.20	2,398.90	1,182.83	60,000.00
CXCL14/BRAK	822.6	1,564.50	1,298.10	902	682.39	150,000.00
MIP-1b	349.2	290.6	4.3	5	3.31	1,500.00
MMP-10	1.2	1.4	90.4	85.4	1.72	3,000.00
MMP-2	5,708.10	6,233.00	843.9	402.4	311.68	150,000.00
MMP-3	13,843.60	13,980.10	19,266.60	9,949.60	120.83	45,000.00
MMP-7	1,221.00	1,316.60	2,930.60	1,452.00	974.10	1,200,000.00
MMP-9	22,069.70	14,406.00	386.7	272.4	11.82	15,000.00
PAI-I	32,243.50	29,660.30	999.5	818.3	198.00	60,000.00
RANK	760.4	734.6	241.5	242.1	242.18	150,000.00
TIMP-1	136,076.60	110,599.80	13,998.10	21,937.50	48.99	60,000.00
VE-Cadherin	31,692.80	29,712.60	2,342.60	2,120.30	2,190.16	300,000.00
6ckine	6,056.60	4,224.00	1,241.20	705.4	888.52	60,000.00
BLC	28.6	36.9	1.2	1	8.04	15,000.00
CXCL16	4,245.20	4,392.20	18.2	160.6	11.52	15,000.00
EGF	776.7	525.2	2	1.8	1.33	600.00
ENA-78	8,010.20	6,807.10	12.3	26.5	23.59	15,000.00
GDF-15	1,013.60	926.3	2.6	6.1	1.80	3,000.00
GM-CSF	16.3	16	1.2	1.8	4.10	1,500.00
IFNg	49.7	39.2	8.2	8	30.76	15,000.00
IL-1a	9.3	9.6	2.4	1.9	6.29	3,000.00
IL-6	40.8	42.4	5.4	5.8	10.42	3,000.00
MCP-1	134.3	106.9	8	7	7.00	3,000.00
MIP-1a	26.8	21.2	8.5	9.2	16.27	15,000.00
OPG	1,010.50	1,021.70	353.8	328.9	31.80	30,000.00
TGF-b1	7,383.70	7,147.00	949.9	898.6	1,240.87	150,000.00
TIMP-2	8,582.90	9,129.90	547.2	2,236.20	10.65	15,000.00
TNFa	307.6	286.8	35	39.3	53.95	3,000.00
VEGF	105.6	76.2	17.6	20.8	5.31	3,000.00
ICAM-1	22,786.40	18,286.20	747.6	814.5	165.84	150,000.00

Table 3.4: Synovial fluid (SF) and plasma biomarkers for which a statistically significant relationship with morphology existed, and their general functions

Biomarker	Protein Family	General Functions
6ckine (CCL21)	Chemokine	responsible for stimulating chemotaxis for thymocytes and activated T-cells[75]
MMP-3, 7 and 9	Matrix Metalloproteinases	involved in the breakdown of ECM in normal and diseased states; degrade proteoglycans, fibronectin, elastin, laminin, collagens III, IV, IX, and X and casein; associated with wound healing[59, 75]
CXCL14 and CXCL16	Chemokines	CXCL14 is a potent chemoattractant for neutrophils, and weaker for dendritic cells.[76] CXCL16 is a strong chemoattractant for macrophages.[77]
ANG (Angiogenin)	Ribonuclease	mediates blood vessel formation; involved in decreasing protein synthesis[75, 78]
ENA-78 (CXCL5)	Chemokine	responsible for neutrophil activation associated with acute inflammatory response[75]
GDF-15	TGF-beta	part of the TGF-beta family; plays a role in regulating inflammatory and apoptotic pathways in injured tissues and during disease processes[75, 79]
TIMP-1	Tissue Inhibitor of Metalloproteinase	a natural inhibitor of MMPs; promotes cell proliferation; "expression from some but not all inactive x-chromosomes suggests that this gene inactivation is polymorphic in human females"[52, 59, 75]

Table 3.5: Additional Plasma biomarkers for which a statistically significant relationship with morphology existed, and their general functions

Biomarker	Protein Family	General Functions
PAI-1 (Plasminogen Activator Inhibitor)	Proteinase inhibitor	An inhibitor of fibrinolysis[75]
VE (vascular endothelium)-Cadherin	Cadherin	A cell-cell adhesion glygoprotein[75]
VEGF (vascular endothelial growth factor)	Growth factor	associated with increased vascular permeability, inducing angiongenesis, vasculogenesis, endothelial cell growth[75]
MIP1b (CCL4)	Chemokine	Chemokinetic and inflammatory functions[75]
EGF	Growth factor	A potent mitogenic factor with a role in growth, proliferation, and differentiation of numerous cell types[75]
GM-CSF	Colony stimulating factor	High affinity receptor for IL-3, IL-5 and CSF[75]
TGFB1	TGF-beta	Regulates proliferation, differentiation, adhesion, migration and other functions in many cell types [75]
IFNg	Interferon	Potent activator of macrophages [75]
TNF-alpha	Tumor Necrosis Factor	Proinflammatory; secreted by macrophages[75]
IL1a	Interleukin	Involved in various inflammatory processes; produced by monocytes and macrophages in response to cell injury[75]
IL6	Interleukin	Functions in inflammation and maturation of B cells; produced at sites of acute and chronic inflammation[75]
BDNF	Growth factor	Induced by cortical neurons; may play a role in the regulation of the stress response[75]

Figure 3.1: The emerging paradigm shift in the understanding, diagnosis, and treatment of OA will integrate the skills of a trained clinician, advanced imaging techniques, and an understanding of effects of biomarkers.

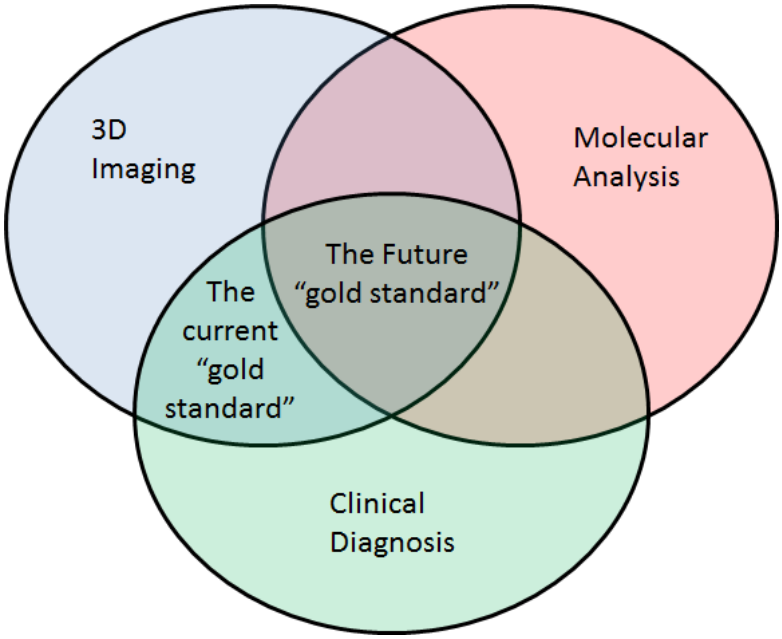

Figure 3.2: a) Average control and OA 3D correspondent models obtained using SPHARM-PDM; b) semitransparent overlays; c) signed difference map between each correspondent point (color map displayed over OA average model)

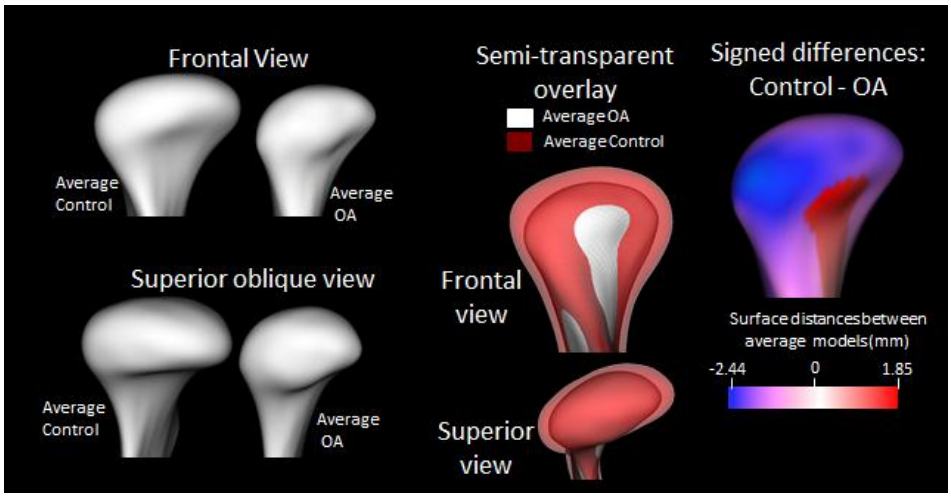

Figure 3.3: Results of Shape Analysis MANCOVA for 10 Proteins in the synovial fluid that presented statistically significant Pearson correlations between biomarker levels and morphology: 6ckine,ANG, CXCL14, CXCL16, ENA-78, GDF15, MMP-3, MMP-7, MMP-9, TIMP-1.

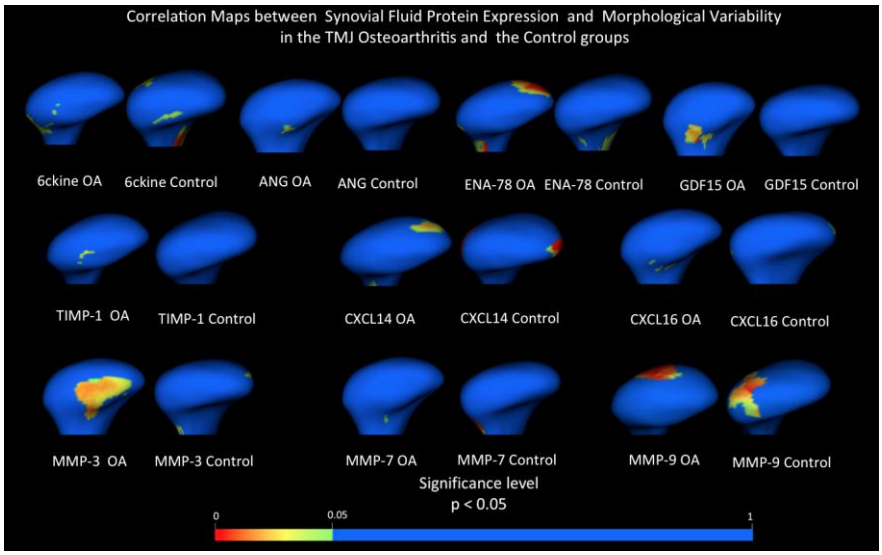

Figure 3.4: Shape Analysis MANCOVA for levels of the same 10 Proteins in figure 3.2 in the plasma that presented significant Pearson correlations between biomarker levels and morphology: 6ckine, ANG, CXCL14, CXCL16, ENA-78, GDF15, MMP-3, MMP-7, MMP-9, TIMP-1.

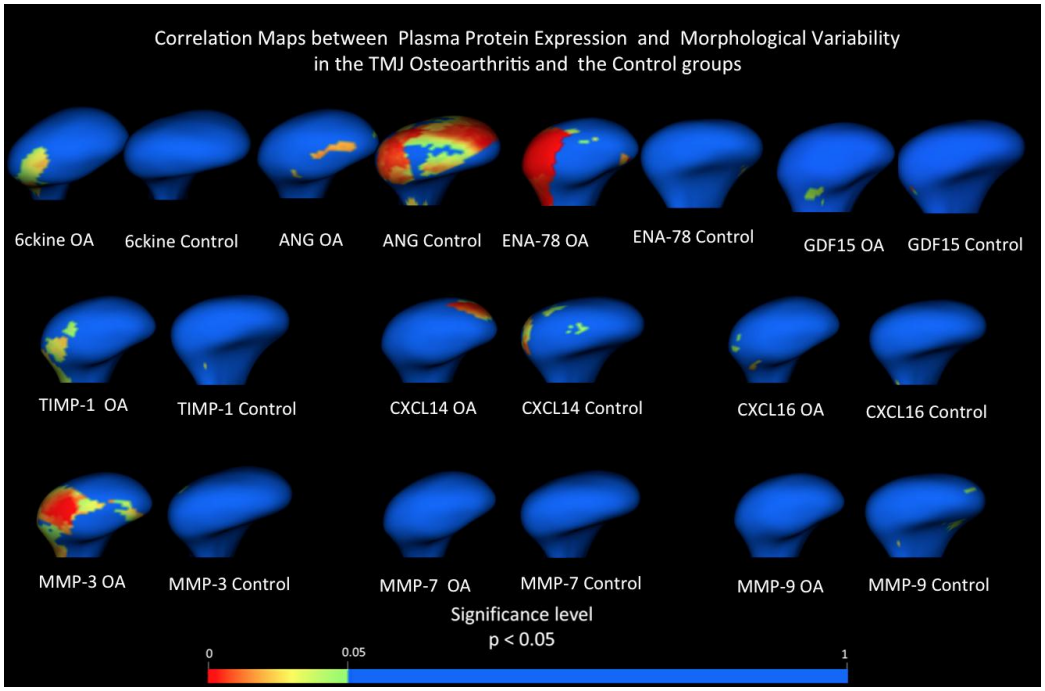

Figure 3.5: Shape Analysis MANCOVA for 12 Proteins in the plasma that presented statistically significant Pearson correlations between biomarker levels and morphology of the superior surface of the lateral pole of the condyle in the OA groups: PAI-1, VE-Cadherin, VEGF, MIP-1b, EGF, GM-CSF, TGFb1, IFNg, TNFa, IL-1a, IL-6, and BDNF .

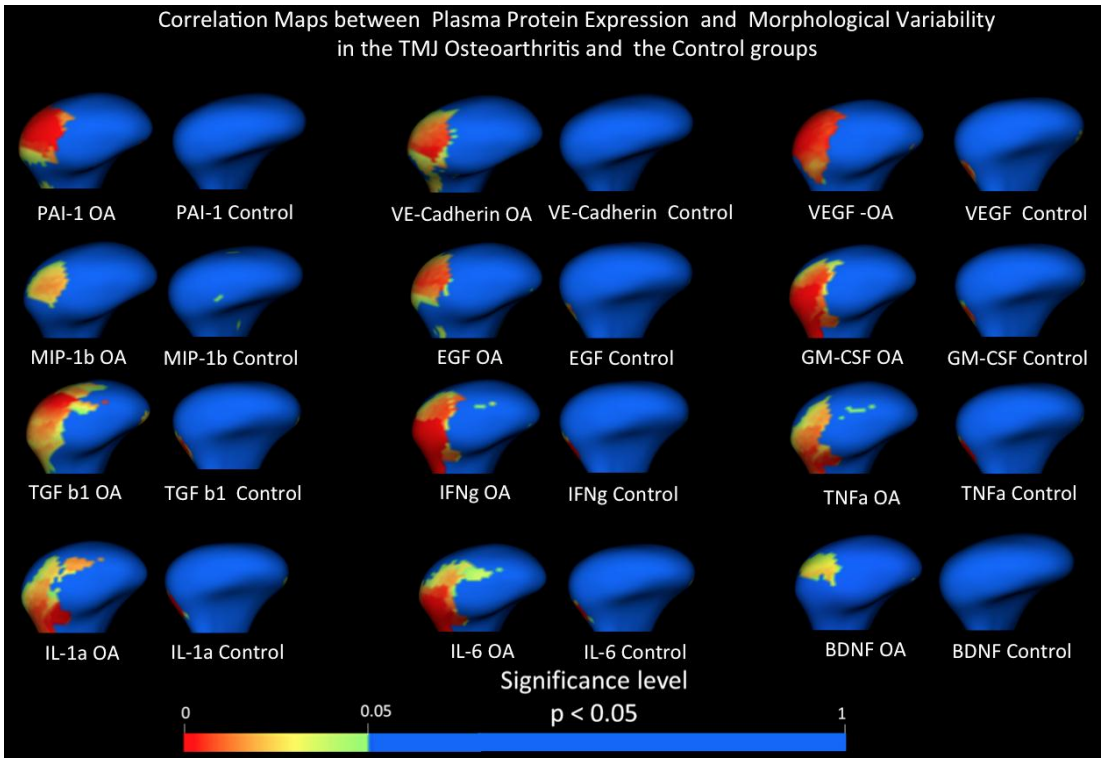

Figure 3.6: Shape Analysis MANCOVA for 12 Proteins that presented statistically significant Pearson correlations at 0.05 corrected with a false discovery rate of 0.2. This means that 20% of significant locations are expected to be false positives, but confirm the overall pattern of the correlations between biomarker levels and morphology in the OA group: ENA-78, PAI-1, VE-Cadherin, VEGF, MMP-3, EGF, GM-CSF, TGFb1, IFNg, TNFa, IL-1a and IL-6. ANG appears to be important in the physiologic remodeling in control subjects.

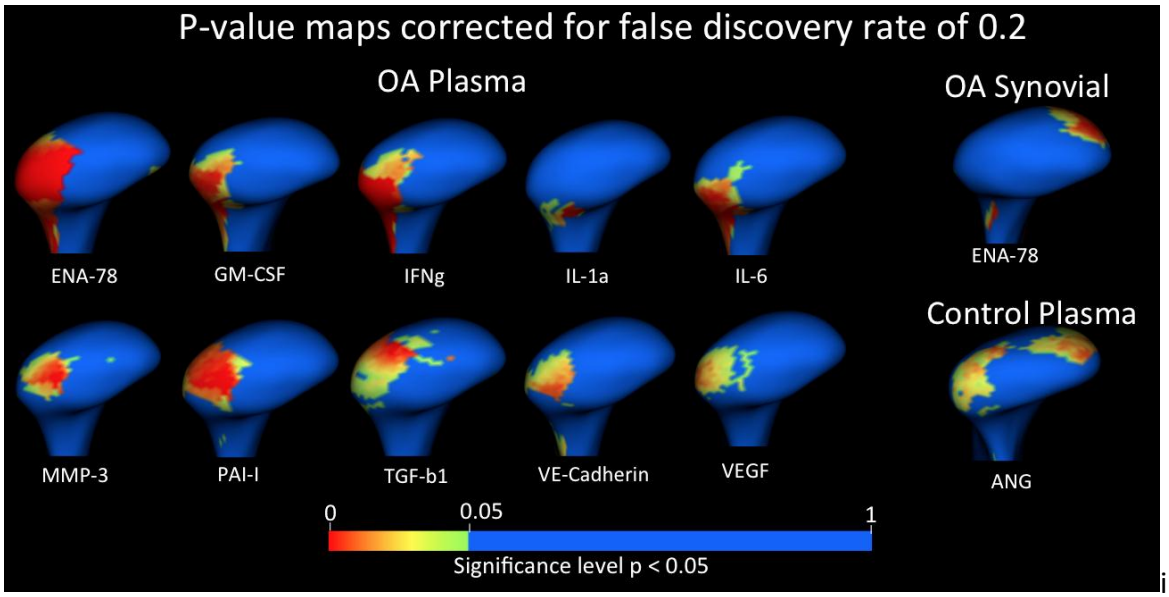

References

1) Hunter, D. J., & Lo, G. H. (2008). The management of osteoarthritis: An overview and call to appropriate conservative treatment. *Rheumatic Diseases Clinics of North America, 34*(3), 689-712. doi:10.1016/j.rdc.2008.05.008.

2) Brandt, K. (2009). Etiopathogenesis of osteoarthritis. *The Medical Clinics of North America, 93*(1) Retrieved from University of North Carol database.

3) Dworkin, S.F., (2010). Research Diagnostic Criteria for Temporomandibular Disorders: Current Status and Future Relevance. *Journal of Oral Rehabilitation, 37*, 734-743.

4) Dworkin, S. F., & LeResche, L. (1992). Research diagnostic criteria for temporomandibular disorders: Review, criteria, examinations and specifications, critique. *Journal of Craniomandibular Disorders : Facial & Oral Pain, 6*(4), 301-355.

5) Look, J. O., John, M. T., Tai, F., Huggins, K. H., Lenton, P. A., Truelove, E. L., et al. (2010). The research diagnostic criteria for temporomandibular disorders: Reliability of axis I diagnoses and selected clinical measures. *Journal of Orofacial Pain, 24*(1), 25-34.

6) Ahmad, M. (2009). Research diagnostic criteria for temporomandibular disorders (RDC/TMD): Development of image analysis criteria and examiner reliability for image analysis. *Oral Surgery, Oral Medicine, Oral Pathology, Oral Radiology and Endodontics, 107*(6), 844-860. Retrieved from University of North Carol database.

7) Centers For Disease Control. (2010). *Arthritis.* Retrieved May/19http://www.cdc.gov/arthritis/data_statistics.htm.

8) Wadhwa, S., & Kapila, S. (2008). TMJ disorders: Future innovations in diagnostics and therapeutics. *Journal of Dental Education, 72*(8), 930-947.

9) LeResche L. Epidemiology of temporomandibular disorders: Implications for the investigation of etiologic factors. Crit Rev Oral Biol Med. 1997;8(3):291-305. Review.

10) Helenius LM, Tervahartiala P, Helenius I, Al-Sukhun J, Kivisaari L, Suuronen R, Kautiainen H, Hallikainen D, Lindqvist C, Leirisalo-Repo M. Clinical, radiographic and MRI findings of the temporomandibular joint in patients with different rheumatic diseases. Int J Oral Maxillofac Surg. 2006;35(11):983-989. Epub 2006 Oct 18. PMID: 17052893.

11) De Leeuw R. American Academy of Orofacial Pain Guidelines for Assessment, Diagnosis, and Management. 4th edition. Chicago: Quintessence Publishing Co; 2008.

12) Gatchel RJ, Stowell AW, Wildenstein L, Riggs R, Ellis E 3rd. Efficacy of an early intervention for patients with acute temporomandibular disorder-related pain: a one-year outcome study. JADA. 2006;137(3):339–47. PMID: 16570467.

13) Alexiou, K., Stamatakis, H., & Tsiklakis, K. (2009). Evaluation of the severity of temporomandibular joint osteoarthritic changes related to age using cone beam computed tomography. *Dento Maxillo Facial Radiology, 38*(3), 141-147. doi:10.1259/dmfr/59263880.

14) Hunter, D. J., McDougall, J. J., & Keefe, F. J. (2009). The symptoms of osteoarthritis and the genesis of pain. *The Medical Clinics of North America, 93*(1), 83-100, xi. doi:10.1016/j.mcna.2008.08.008.

15) McDougall, J. J., Andruski, B., Schuelert, N., Hallgrimsson, B., & Matyas, J. R. (2009). Unravelling the relationship between age, nociception and joint destruction in naturally occurring osteoarthritis of dunkin hartley guinea pigs. *Pain, 141*(3), 222-232. doi:10.1016/j.pain.2008.10.013.

16) Kubassova, O., Boesen, M., Peloschek, P., Langs, G., Cimmino, M. A., Bliddal, H., et al. (2009). Quantifying disease activity and damage by imaging in rheumatoid arthritis and osteoarthritis. *Annals of the New York Academy of Sciences, 1154*, 207-238. doi:10.1111/j.1749-6632.2009.04392.x.

17) Cevidanes, L. (2010). Quantification of condylar resorption in temporomandibular joint osteoarthritis. *Oral Surgery, Oral Medicine, Oral Pathology, Oral Radiology and Endodontics, 110*, 110-117. Retrieved from University of North Carol database.

18) Barghan, S., Merrill, R., & Tetradis, S. (2010). Cone beam computed tomography imaging in the evaluation of the temporomandibular joint. *Journal of the California Dental Association, 38*(1), 33-39.

19) Wiese, M., Svensson, P., Bakke, M., List, T., Hintze, H., Petersson, A., et al. (2008). Association between temporomandibular joint symptoms, signs, and clinical diagnosis using the RDC/TMD and radiographic findings in temporomandibular joint tomograms. *Journal of Orofacial Pain, 22*(3), 239-251.

20) B Paniagua, L Cevidanes, D Walker, et al.,. (2011). Clinical application of SPHARM-PDM to quantify temporomandibular joint osteoarthritis. *Computerized Medical Imaging and Graphics,* Retrieved from University of North Carol database.

21) Honey, O. B., Scarfe, W. C., Hilgers, M. J., Klueber, K., Silveira, A. M., Haskell, B. S., et al. (2007). Accuracy of cone-beam computed tomography imaging of the temporomandibular joint: Comparisons with panoramic radiology and linear tomography. *American Journal of Orthodontics and Dentofacial Orthopedics : Official Publication of the American Association of Orthodontists, its Constituent Societies, and the American Board of Orthodontics, 132*(4), 429-438. doi:10.1016/j.ajodo.2005.10.032.

22) Walker D, Cevidanes LHS, & Lim PF. (2008a). Condylar remodeling in temporomandibular disorder using 3D surface models analysis of condylar [Abstract]. *Jounral of Dental Research, 87*(Special Issue A) 82.

23) Walker DG, Cevidanes LHS, Lim PF, Styner M, Phillips C. (2008). Condylar morphology in temporomandibular disorder using 3D shape analysis [Abstract]. *Journal of Dental Research, 87*(Special Issue B) 022.

24) Wiese, M., Wenzel, A., et al. (2008). Osseous Changes and Condyle Position in TMJ Tomograms: Impact of RDC/TMD Clinical Diagnoses on Agreement Between Expected and Actual Findings. Oral Surg Oral Med Oral Pathol Oral Radiol Endod, 106: e52-e63.

25) Walker D, Cevidanes L, Paniagua B, Zhu H, Styner M, Lim PF. (2010). Validation of shape correspondence for quantification of condylar resorption [Abstract]. *Jounral of Dental Research, 89*(Special Issue A) 1200.

26) Walker DG, Cevidanes LHS, Lim PF, Ludlow J, Styner M, Phillips C. (2009). Pain correlations to 3D condylar morphology in temporomandibular disorder [Abstract]. *Journal of Dental Research, 88*(Special Issue A) 439.

27) Neuroimaging Informatics Tools and Resources Clearinghouse (NITRC) (2012). *SPHARM-PDM Toolbox*. Retrieved Jan/20 www.nitrc.org/projects/spharm-pdm.

28) Insight Segmentation and Registration Tookit (ITK) (2013). Retrieved Jan/20 www.itk.org.

29) Styner M, Oguz I, Xu S, Brechbuhler C, Pantazis D, Levitt J, Shenton ME, Gerig G. (2006). Framework for the statistical shape analysis of brain structures using spharm-PDM. *Insight Journal*, 1.

30) Neuroimaging Informatics Tools and Resources Clearinghouse (NITRC) (2013). shapeAnalysisMANCOVA – SPHARM tools. Retrieved Jan/20 http://www.nitrc.org/projects/shape_mancova/.

31) DC Bauer, DJ Hunter, SB Abramson, et al. (2006). Review: Classification of osteoarthritis biomarkers: A proposed approach. *Osteoarthritis and Cartilage, 14*, 723-727. Retrieved from University of North Carol database.

32) Hayami T, Pickarski M, Wesolowski GA, McLane J, Bone A, Destefano J, Rodan GA, Duong le T. (2004). The role of subchondral bone remodeling in osteoarthritis: reduction of cartilage degeneration and prevention of osteophyte formation by alendronate in the rat anterior cruciate ligament transection model. *Arthritis Rheum*. Apr;50(4):1193-206.

33) S.B. Abramson, M. Attur. Developments in the scientific understanding of osteoarthritis Arthritis Res Ther, 11 (2009), p. 227.

34) M.A. Karsdal, T.J. Martin, J. Bollerslev, C. Christiansen, K. Henriksen Are nonresorbing osteoclasts sources of bone anabolic activity? JBMR, 22 (2007), pp. 487–494.

35) Wieland HA, Michaelis M, Kirschbaum BJ, Rudolphi KA . Osteoarthritis - an untreatable disease? *Nat Rev Drug Discov*. 2005 Apr;4(4):331-44. Review.

36) Kraus, V. B., Nevitt, M., & Sandell, L. J. (2010). Summary of the OA biomarkers workshop 2009--biochemical biomarkers: Biology, validation, and clinical studies. *Osteoarthritis and Cartilage / OARS, Osteoarthritis Research Society, 18*(6), 742-745. doi:10.1016/j.joca.2010.02.014.

37) Edmonds, S. (2009). Therapeutic targets for osteoarthritis. *Maturitas, 63*(3), 191-194. doi:10.1016/j.maturitas.2009.03.015.

38) Williams, F. M. (2009). Biomarkers: In combination they may do better. *Arthritis Research & Therapy, 11*(5), 130. doi:10.1186/ar2839.

39) Zhang, Y., & Jordan, J. M. (2010). Epidemiology of osteoarthritis. *Clinics in Geriatric Medicine, 26*(3), 355-369. doi:10.1016/j.cger.2010.03.001.

40) Dam, E. B., Loog, M., Christiansen, C., Byrjalsen, I., Folkesson, J., Nielsen, M., et al. (2009). Identification of progressors in osteoarthritis by combining biochemical and MRI-based markers. *Arthritis Research & Therapy, 11*(4), R115. doi:10.1186/ar2774.

41) Addison, S., Coleman, R. E., Feng, S., McDaniel, G., & Kraus, V. B. (2009). Whole-body bone scintigraphy provides a measure of the total-body burden of osteoarthritis for the purpose of systemic biomarker validation. *Arthritis and Rheumatism, 60*(11), 3366-3373. doi:10.1002/art.24856.

42) Koyama, J., Nishiyama, H., & Hayashi, T. (2007). Follow-up study of condylar bony changes using helical computed tomography in patients with temporomandibular disorder. *Dento Maxillo Facial Radiology, 36*(8), 472-477. doi:10.1259/dmfr/28078357.

43) Yamada, K., Hiruma, Y., Hanada, K., Hayashi, T., Koyama, J., & Ito, J. (1999). Condylar bony change and craniofacial morphology in orthodontic patients with temporomandibular disorders (TMD) symptoms: A pilot study using helical computed tomography and magnetic resonance imaging. *Clinical Orthodontics and Research, 2*(3), 133-142.

44) Yamada, K., Hanada, K., Hayashi, T., & Ito, J. (2001). Condylar bony change, disk displacement, and signs and symptoms of TMJ disorders in orthognathic surgery patients. *Oral Surgery, Oral Medicine, Oral Pathology, Oral Radiology, and Endodontics, 91*(5), 603-610. doi:10.1067/moe.2001.112153.

45) Schiffman, E. L., Ohrbach, R., Truelove, E. L., Tai, F., Anderson, G. C., Pan, W., et al. (2010). The research diagnostic criteria for temporomandibular disorders. V: Methods used to establish and validate revised axis I diagnostic algorithms. *Journal of Orofacial Pain, 24*(1), 63-78.

46) Truelove, E., Pan, W., Look, J. O., Mancl, L. A., Ohrbach, R. K., Velly, A. M., et al. (2010). The research diagnostic criteria for temporomandibular disorders. III: Validity of axis I diagnoses. *Journal of Orofacial Pain, 24*(1), 35-47.

47) Schiffman, E. L., Truelove, E. L., Ohrbach, R., Anderson, G. C., John, M. T., List, T., et al. (2010). The research diagnostic criteria for temporomandibular disorders. I: Overview and methodology for assessment of validity. *Journal of Orofacial Pain, 24*(1), 7-24.

48) Cevidanes LHS, Walker D, Styner M, Lim PF. (2008). Condylar resorption in patients with TMD. In McNamara Jr JA, Kapila SD. (Ed.), *Temporomandibular disorders and orofacial pain - separating controversy from consensus* (pp. 147).

49) van Spil, W. E., DeGroot, J., Lems, W. F., Oostveen, J. C., & Lafeber, F. P. (2010). Serum and urinary biochemical markers for knee and hip-osteoarthritis: A systematic review applying the consensus BIPED criteria. *Osteoarthritis and Cartilage / OARS, Osteoarthritis Research Society, 18*(5), 605-612. doi:10.1016/j.joca.2010.01.012.

50) Ruiz-Romero, C., & Blanco, F. J. (2010). Proteomics role in the search for improved diagnosis, prognosis and treatment of osteoarthritis. *Osteoarthritis and Cartilage / OARS, Osteoarthritis Research Society, 18*(4), 500-509. doi:10.1016/j.joca.2009.11.012.

51) Anitua, E. (2009). Relationship between investigative biomarkers and radiographic grading in patients with knee osteoarthritis. *Internal Journal of Rheumatology,* Retrieved from University of North Carol database.

52) Ling, S. M., Patel, D. D., Garnero, P., Zhan, M., Vaduganathan, M., Muller, D., et al. (2009). Serum protein signatures detect early radiographic osteoarthritis.

Osteoarthritis and Cartilage / OARS, Osteoarthritis Research Society, 17(1), 43-48. doi:10.1016/j.joca.2008.05.004.

53) Diatchenko, L., Nackley, A., & et al. (2007). Genetic architecture of human pain perception. *Trends in Genetics, 23*(12), 605-613.

54) Goldring, M. B., & Goldring, S. R. (2007). Osteoarthritis. *Journal of Cellular Physiology, 213*(3), 626-634. doi:10.1002/jcp.21258.

55) Hajati, A. (2009). Endogenous glutamate in association with inflammatory and hormonal factors modulates bone tissue resorption of the temporomandibular joint in patients with early rheumatoid arthritis. *Journal of Oral and Maxillofacial Surgery, 67*, 1895-1903. Retrieved from University of North Carol database.

56) Kidd, B. L., Photiou, A., & Inglis, J. J. (2004). The role of inflammatory mediators on nociception and pain in arthritis. *Novartis Foundation Symposium, 260*, 122-33; discussion 133-8, 277-9.

57) Marshall, K. W., Zhang, H., Yager, T. D., Nossova, N., Dempsey, A., Zheng, R., et al. (2005). Blood-based biomarkers for detecting mild osteoarthritis in the human knee. *Osteoarthritis and Cartilage / OARS, Osteoarthritis Research Society, 13*(10), 861-871. doi:10.1016/j.joca.2005.06.002.

58) Ohno, S., Schmid, T., Tanne, Y., Kamiya, T., Honda, K., Ohno-Nakahara, M., et al. (2006). Expression of superficial zone protein in mandibular condyle cartilage. *Osteoarthritis and Cartilage / OARS, Osteoarthritis Research Society, 14*(8), 807-813. doi:10.1016/j.joca.2006.02.002.

59) Rousseau, J. C., & Delmas, P. D. (2007). Biological markers in osteoarthritis. *Nature Clinical Practice.Rheumatology, 3*(6), 346-356. doi:10.1038/ncprheum0508.

60) Slade GD, Conrad MS, Diatchenko L, Rashid NU, Zhong S, Smith S, Rhodes J, Medvedev A, Makarov S, Maixner W, Nackley AG. Cytokine biomarkers and chronic pain: association of genes, transcription, and circulating proteins with temporomandibular disorders and widespread palpation tenderness. *Pain*. 2011 Dec;152(12):2802-12.

61) Dinarello CA . Proinflammatory cytokines. *Chest.* 2000 Aug;118(2):503-8. Review.

62) Samuels, J., Krasnokutsky, S., & Abramson, S. B. (2008). Osteoarthritis: A tale of three tissues. *Bulletin of the NYU Hospital for Joint Diseases, 66*(3), 244-250.

63) van Spil, Jansen, Bijlsma, Reijman, DeGroot, Welsing, Lafeber . Clusters within a wide spectrum of biochemical markers for OA: data from CHECK, a large cohort of individuals with very early symptomatic OA. Osteoarthritis Cartilage. 2012 Jul;20(7):745-54.

64) Cevidanes, L. (2010). Quantification of condylar resorption in temporomandibular joint osteoarthritis. *Oral Surgery, Oral Medicine, Oral Pathology, Oral Radiology and Endodontics, 110*, 110-117. Retrieved from University of North Carol database.

65) Nordahl, S., Alstergren, P., Eliasson, S., & Kopp, S. (1998). Interleukin-1beta in plasma and synovial fluid in relation to radiographic changes in arthritic temporomandibular joints. *European Journal of Oral Sciences, 106*(1), 559-563.

66) Alstergren, P. (1997). Pain and synovial fluid concentration of serotonin in arthritic tempormandibular joints. *Pain (Amsterdam), 72*, 137-143. Retrieved from University of North Carol database.

67) Alstergren, P. (2000). Cytokines in temporomandibular joint arthritis. *Oral Diseases, 6*, 331-334. Retrieved from University of North Carol database.

68) Nordahl, S., Alstergren, P., & Kopp, S. (2000). Tumor necrosis factor-alpha in synovial fluid and plasma from patients with chronic connective tissue disease and its relation to temporomandibular joint pain. *Journal of Oral and Maxillofacial Surgery : Official Journal of the American Association of Oral and Maxillofacial Surgeons, 58*(5), 525-530.

69) Alstergren, P. (2000). Prostaglandin E2 in temporomandibular joint synovial fluid and its relation to pain and inflammatory disorders. *Journal of Oral and Maxillofacial Surgery, 58*, 180-186. Retrieved from University of North Carol database.

70) Alstergren, P., Kopp, S., & Theodorsson, E. (1999). Synovial fluid sampling from the temporomandibular joint: Sample quality criteria and levels of interleukin-1 beta and serotonin. *Acta Odontologica Scandinavica, 57*(1), 16-22.

71) Alstergren, P. (1998). Interleukin-1B in synovial fluid from the arthritic temporomandibular joint and its relation to pain, mobility, and anterior open bite. *Journal of Oral and Maxillofacial Surgery, 56*, 1059-1065. Retrieved from University of North Carol database.

72) Alstergren, P., Appelgren, A., Appelgren, B., Kopp, S., Lundeberg, T., & Theodorsson, E. (1996). The effect on joint fluid concentration of neuropeptide Y by intra-articular injection of glucocorticoid in temporomandibular joint arthritis. *Acta Odontologica Scandinavica, 54*(1), 1-7.

73) Alstergren, P., Appelgren, A., Appelgren, B., Kopp, S., Lundeberg, T., & Theodorsson, E. (1995). Co-variation of neuropeptide Y, calcitonin gene-related peptide, substance P and neurokinin A in joint fluid from patients with temporomandibular joint arthritis. *Archives of Oral Biology, 40*(2), 127-135.

74) RayBiotech. (2012) *Quantibody Arrays.* Retrieved December, 19, 2012. http://www.raybiotech.com/quantibody-en-2.html.

75) NCBI Gene Database [Internet]. Bethesda, MD: National Center for Biotechnology Information, U.S. National Library of Medicine. [cited 2012 Dec 19]. Available from: http://www.ncbi.nlm.nih.gov/gene.

76) Chen L, Guo L, Tian J, He H, Marinova E, Zhang P, Zheng B, Han S. Overexpression of CXC chemokine ligand 14 exacerbates collagen-induced arthritis. *J Immunol*. 2010 Apr 15;184(8):4455-9

77) Smith H, Whittall C, Weksler B, Middleton J. Chemokines stimulate bidirectional migration of human mesenchymal stem cells across bone marrow endothelial cells. *Stem Cells Dev*. 2012 Feb 10;21(3):476-86

76) Matsumoto K, Honda K, Ohshima M, Yamaguchi Y, Nakajima I, Micke P, Otsuka K. Cytokine profile in synovial fluid from patients with internal derangement of the temporomandibular joint: a preliminary study. Dentomaxillofac Radiol. 2006;35(6):432-41.

77) Zimmers T, Jin X, Hsiao E, McGrath S, Esquela A, Koniaris L (2005). Growth differentiation factor-15/macrophage inhibitory cytokine-1 induction after kidney and lung injury. *Shock* **23** (6): 543–8.

78) Matloubian M, David A, Engel S, Ryan J, Cyster J (2000). A transmembrane CXC chemokine is a ligand for HIV-coreceptor Bonzo. *Nat Immunol* **1** (4): 298–304.

79) Pierer M, Rethage J, Seibl R, Lauener R, Brentano F, Wagner U, et al. (2004). Chemokine Secretion of Rheumatoid Arthritis Synovial Fibroblasts Stimulated by Toll-like Receptor 2 Ligands. J Immunol 172 (2): 1256-65.